

An extremely peculiar hot subdwarf with a ten-thousand-fold excess of zirconium, yttrium, and strontium.

Naslim N.^{1*}, C.S. Jeffery^{1†}, N.T. Behara^{1,2} & A. Hibbert³

¹Armagh Observatory, College Hill, Armagh BT61 9DG

²Institut d’Astronomie et d’Astrophysique, Université Libre de Bruxelles, Belgium

³School of Mathematics and Physics, Queens University Belfast, Belfast BT1 7NN

Accepted Received ; in original form

ABSTRACT

Helium-rich subdwarf B (He-sdB) stars represent a small group of low-mass hot stars with luminosities greater than those of conventional subdwarf B stars, and effective temperatures lower than those of subdwarf O stars. By measuring their surface chemistry, we aim to explore the connection between He-sdB stars, He-rich sdO stars and normal sdB stars.

LS IV–14°116 is a relatively intermediate He-sdB star, also known to be a photometric variable. High-resolution blue-optical spectroscopy was obtained with the Anglo-Australian Telescope. Analysis of the spectrum shows LS IV–14°116 to have effective temperature $T_{\text{eff}} = 34\,000 \pm 500\text{K}$, surface gravity $\log g = 5.6 \pm 0.2$, and surface helium abundance $n_{\text{He}} = 0.16 \pm 0.03$ by number. This places the star slightly above the standard extended horizontal branch, as represented by normal sdB stars. The magnesium and silicon abundances indicate the star to be metal poor relative to the Sun.

A number of significant but unfamiliar absorption lines were identified as being due to germanium, strontium, yttrium and zirconium. After calculating oscillator strengths (for Ge, Y and Zr), the photospheric abundances of these elements were established to range from 3 dex (Ge) to 4 dex (Sr, Y and Zr) above solar. The most likely explanation is that these overabundances are caused by radiatively-driven diffusion forming a chemical cloud layer in the photosphere. It is conjectured that this cloud formation could be mediated by a strong magnetic field.

Key words: stars: evolution, stars: mass-loss, stars: chemically peculiar

1 INTRODUCTION

Subdwarf B stars are low-mass core helium burning stars with extremely thin hydrogen envelopes. They behave as helium main-sequence stars of roughly half a solar mass. Their atmospheres are generally helium deficient; radiative levitation and gravitational settling combine to make helium sink below the hydrogen-rich surface (Heber 1986), to deplete other light elements, and to enhance abundances of heavy elements in the photosphere (O’Toole & Heber 2006).

However, almost 5% of the total subdwarf population comprise stars with helium-rich atmospheres (Green et al. 1986; Ahmad & Jeffery 2006). They have been variously classified as sdOB, sdOC and sdOD (Green et al. 1986) stars, but more recently as He-sdB and He-sdO stars (Moehler et al. 1990; Ahmad & Jeffery 2004). Their optical spectra are characterised by strong HeI (He-sdB) and HeII (He-sdO) lines.

LS IV–14°116 was classified as an sdO star by Kilkenney & Pauls (1990) and as an He-rich sdO star by Viton et al. (1991). Jeffery et al. (1996) included this star in their catalogue of He-sdB stars. Ahmad & Jeffery (2005) reported pulsations in LS IV–14°116 with periods of 1950 and 2900 s, the first discovery of pulsation in a He-sdB star. However, it is only mildly helium rich, with $n_{\text{He}} \approx 0.2$ (Ahmad & Jeffery 2003).

This paper reports the first detailed abundance analysis of LS IV–14°116 using high resolution optical spectroscopy. In particular, it reports the first discovery of strontium, germanium, yttrium and zirconium in the optical spectrum of a hot subdwarf.

2 OBSERVATIONS

Three spectra of LS IV–14°116 were obtained with the University College London Echelle Spectrograph (UCLES) on the Anglo-Australian Telescope (AAT) on 2005 August 26. Each exposure was 1800 s in duration. The observations were obtained, reduced and analyzed in the same way as described by Naslim et al. (2010).

* E-mail: nas@arm.ac.uk

† E-mail: csj@arm.ac.uk

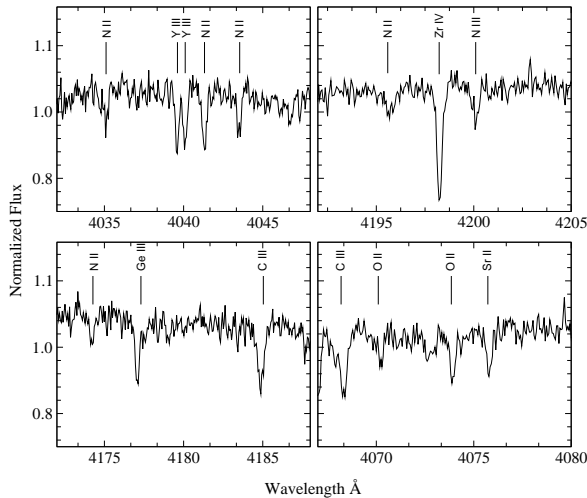


Figure 1. Y III, Zr IV, Sr II and Ge III lines in LS IV–14° 116.

The AAT/UCLES spectrum of LS IV–14° 116 shows N II, N III, C II, C III, O II, Si III, and Mg II lines, together with strong He I and He II λ 4686. Unlike other He-sdB stars, the spectrum displays relatively strong hydrogen Balmer lines. While analysing this spectrum we noted a number of strong unidentified lines. Using the NIST database of atomic spectra, we discovered that these lines are due to Zr IV, Y III, Ge III and Sr II (Fig. 1). As far as we know, Zr IV, Y III, and Ge III have not been identified in any other ground-based astronomical spectrum, although Zr and Ge have been observed with large overabundances in ultraviolet spectra of sdB stars (O’Toole 2004; O’Toole & Heber 2006; Chayer et al. 2006; Blanchette et al. 2008). The Sr II resonance lines are seen in chemically peculiar late-B stars (HgMn stars, for example), but are completely unknown at late-O or early-B spectral types. These line identifications immediately pointed to a remarkable chemical anomaly in this star. However, the anomaly could not be measured immediately, since no oscillator strengths existed for the optical Zr IV, Y III, and Ge III lines.

We have not identified lines for any iron-group elements in this spectrum. There remain a small number of lines which we have been unable to identify. The most notable have wavelengths 4007.40 Å and 4216.20 Å with equivalent widths 40 and 34 mÅ, respectively.

3 PHYSICAL PARAMETERS OF LS IV–14° 116

We measured the effective temperature T_{eff} , surface gravity $\log g$, and elemental abundances of LS IV–14° 116 using the same method as described by Naslim et al. (2010). We found the microturbulent velocity $v_t = 10 \text{ km s}^{-1}$ by minimising the dispersion on carbon abundance measured from six C III absorption lines; adopting $v_t = 5 \text{ km s}^{-1}$ increases this dispersion by 25%. The grids of model atmospheres adopted for analysis were computed with 1/10 solar metallicity, relative helium abundances $n_{\text{He}} = 0.10, 0.20$ and 0.50 by number, and microturbulent velocity $v_t = 10 \text{ km s}^{-1}$.

T_{eff} and $\log g$ were measured using ionisation equilibrium and line profile fitting. Using appropriate model atmospheres, the ionisation equilibrium was established by balancing the abundances determined from N II and N III and from C II and C III lines in the spectrum, as well as by fitting the equivalent width of the temperature

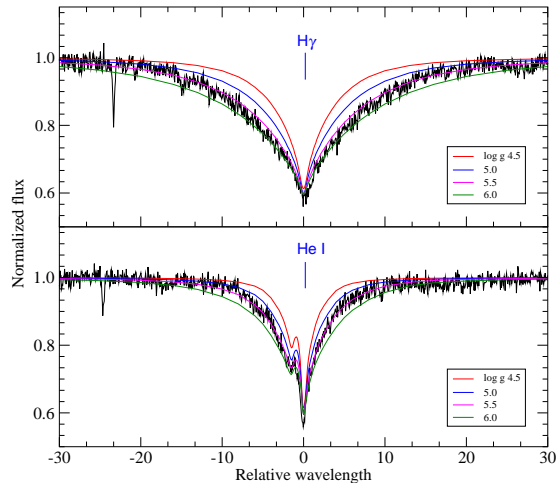


Figure 2. Theoretical line profile fits to He I 4471 and H γ in LS IV–14° 116 for model atmospheres with $n_{\text{He}} = 0.100$, $T_{\text{eff}} = 34\,000 \text{ K}$ and $\log g = 4.5(0.5)6.0$.

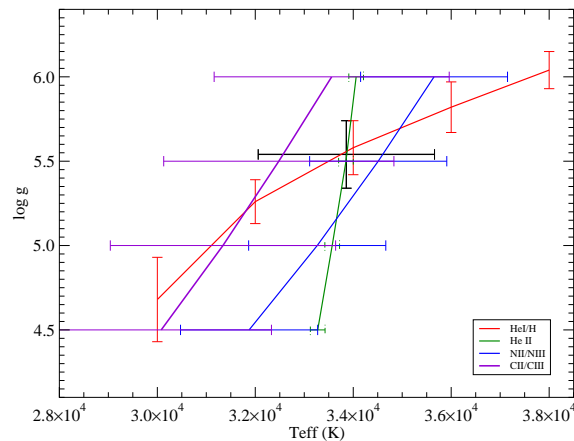


Figure 3. The loci of ionization equilibria for C II/C III, N II/N III and He I, the profile fits to He I and H lines, and the adopted solution.

sensitive He II 4686 line. The surface gravity was established by fitting theoretical profiles to H β , γ , and δ , and to He I 4471 (Fig. 2). The coincidence of profile fits and ionisation equilibria was used to determine the overall solution illustrated in Fig. 3.

We also measured the physical parameters T_{eff} , $\log g$ and helium abundance n_{He} using the package SFIT which finds the best-fit solution within a grid of synthetic spectra. The model grid was defined with $T_{\text{eff}} = 32\,000$ (2000) 38 000 K, $\log g = 4.50(0.5)6.00$, $n_{\text{He}} = 0.10, 0.20, 0.30, 0.50$ and $v_t = 10 \text{ km s}^{-1}$.

Table 1. Atmospheric parameters

| T_{eff} (K) | $\log g$ | n_{He} | Source |
|----------------------|----------------|------------------|------------------------|
| $34\,000 \pm 500$ | 5.6 ± 0.1 | 0.160 ± 0.03 | SFIT |
| $33\,860 \pm 1\,800$ | 5.54 ± 0.2 | | Ion eq |
| $33\,000 \pm 1\,000$ | 5.8 ± 0.2 | 0.2 | Viton et al. (1991) |
| $32\,500 \pm 150$ | 5.4 ± 0.1 | 0.21 | Ahmad & Jeffery (2003) |

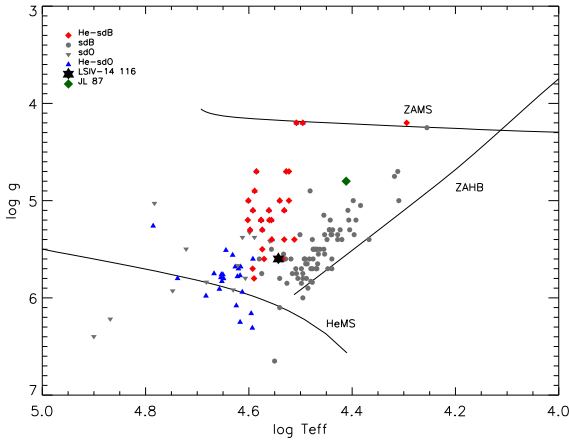


Figure 4. The location of LS IV-14°116 on the $\log g - T_{\text{eff}}$ diagram, compared with normal sdB stars (Edelmann et al. 2003) helium-rich sdB stars (Ahmad & Jeffery 2003; Naslim et al. 2010), helium-rich sdO stars (Stroeer et al. 2007), and JL 87 (Ahmad et al. 2007). A zero-age main sequence ($Y = 0.28, Z = 0.02$), a zero-age horizontal branch ($M_c = 0.485M_{\odot}, Y_e = 0.28, Z = 0.02$) and a helium main sequence ($Z = 0.02$) are also shown.

The observed spectrum of LS IV-14°116 is shown along with the best fit model spectrum in Fig. 5.

The atmospheric properties of LS IV-14°116 deduced from these measurements are given in Table 1. **The projected rotational line broadening measured from ZrIV lines 4198.26Å and 4317.08Å is $v \sin i < 2 \text{ km s}^{-1}$.** SFIT and ionization equilibrium results agree to within the formal errors. Although all ionisation equilibria and profile fits do not converge on a single point, the intersections lie within 3200 K in T_{eff} and 0.5 in $\log g$. We took a weighted mean of these intersections to determine the ionization T_{eff} and $\log g$. For subsequent abundance measurements, we adopted the grid model atmosphere with $T_{\text{eff}} = 34\,000 \text{ K}$, $\log g = 5.5$, $n_{\text{He}} = 0.20$ and $v_t = 10 \text{ km s}^{-1}$.

In view of the atmospheric abundances reported below, the above procedure was repeated with a grid of models in which the abundances of all metals with atomic number ≥ 20 (calcium) except iron were increased to 10 times the solar value. This has proved to be a successful strategy for the analysis of normal sdB star spectra (O’Toole & Heber 2006; Pereira 2010). However in this case, a) we failed to find any agreement between HeII4686 and the NII/III ionisation equilibrium, b) we found the depth of the theoretical H and HeI lines to be consistently deeper than observed and c) whilst leading to a 2000 K reduction in T_{eff} , the new models also led to a significant increase in the measured strontium abundance. Without further diagnostics of high-Z abundances and chemical stratification, the 1/10 solar metallicity models were deemed satisfactory for the present paper.

4 ATOMIC DATA

In order to measure elemental abundances for all visible species, we measured equivalent widths of lines of CII, CIII, NII, NIII, OII, MgII, SiIII, SrII, GeII, YIII and ZrIII. Atomic data and oscillator strengths for most of these lines were available in our own compilation (see Table 2), but data for Sr, Ge, Y and Zr were not.

The atomic data for the relevant transitions of these ions are displayed in Table 3. The labels of the upper and lower states of

Table 2. Individual line equivalent widths W_{λ} and abundances ϵ_i , with adopted oscillator strengths gf , for LS IV-14°116.

| Ion | $\lambda/\text{Å}$ | $\log gf$ | $W_{\lambda}/\text{mÅ}$ | ϵ_i |
|-------|--------------------|-----------|-------------------------|--------------|
| CII | | | | |
| | 4074.48 | 0.204 | 42 | 8.20 |
| | 4074.52 | 0.408 | | |
| | 4074.85 | 0.593 | 57 | 8.08 |
| | 4075.85 | 0.756 | | |
| | 4075.94 | -0.076 | 130 | 7.80 |
| | 4267.02 | 0.559 | | |
| | 4267.27 | 0.734 | | |
| CIII | | | | |
| | 4067.94 | 0.827 | 60 | 7.70 |
| | 4068.91 | 0.945 | 59 | 7.69 |
| | 4070.26 | 1.037 | 82 | 8.37 |
| | 4186.90 | 0.924 | 76 | 8.34 |
| | 4647.42 | 0.072 | 130 | 8.08 |
| | 4650.25 | -0.149 | 98 | 8.01 |
| | 4651.47 | -0.625 | 54 | 7.99 |
| NII | | | | |
| | 3995.00 | 0.225 | 47 | 7.65 |
| | 4041.31 | 0.830 | 45 | 7.82 |
| | 4043.53 | 0.714 | 46 | 7.95 |
| | 4236.86 | 0.396 | 73 | 8.19 |
| | 4236.98 | 0.567 | | |
| | 4241.78 | 0.728 | 35 | 7.85 |
| | 4241.79 | 0.710 | | |
| | 4447.03 | 0.238 | 48 | 8.04 |
| | 4601.48 | -0.385 | 35 | 8.15 |
| | 4607.16 | -0.483 | 42 | 8.35 |
| | 4630.54 | 0.093 | 50 | 7.88 |
| NIII | | | | |
| | 4640.64 | 0.140 | 77 | 8.19 |
| | 4634.14 | -0.108 | 51 | 8.13 |
| OII | | | | |
| | 4072.15 | 0.545 | 21 | 7.42 |
| | 4414.90 | 0.210 | 33 | 7.63 |
| | 4416.97 | -0.041 | 26 | 7.75 |
| MgII | | | | |
| | 4481.13 | 0.568 | 25 | 6.85 |
| SiIII | | | | |
| | 4552.62 | 0.283 | 29 | 6.32 |

gf values: CII Yan et al. (1987), CIII Hibbert (1976); Hardorp & Scholz (1970); Bockasten (1955), NII Becker & Butler (1989), NIII Butler (1984), OII Becker & Butler (1988), SiIII Becker & Butler (1990), MgII Wiese et al. (1966)

each transition include, in addition to the angular momenta and parity, the electron occupancy of the valence subshells, as given by the Hartree-Fock approximation. In practice, the Hartree-Fock (HF) approximation is not sufficiently adequate for the calculation of oscillator strengths, as demonstrated by the work of Brage et al. (1998) for SrII. Instead, each wave function needs to be represented by a configuration interaction (CI) expansion, though the dominant (largest CI mixing coefficient) remains the HF configuration in all the cases considered here, and therefore constitutes an appropriate part of the label.

For the SrII transitions, we have merely quoted the oscillator strength results of Brage et al. (1998), since their work is a substantial MCHF calculation and their final results agree well with the experimental studies of Grevesse et al. (1991) and even with the conceptually simpler calculation of Migdalek & Bayliss (1979) who represented core polarisation by model potentials rather than

Table 3. Atomic data for optical lines of Sr, Ge, Y and Zr, and abundances derived for LS IV–14° 116.

| Ion | $\lambda/\text{\AA}$ | Configuration | E_i/eV | Ref | $\log gf$ | Ref | $w_\lambda/\text{m\AA}$ | ϵ_i |
|-------|----------------------|----------------------------------|-----------------|-----|-----------|-----|-------------------------|--------------|
| SrII | | | | | | | | |
| | 4077.71 | $5s^2 S_{1/2} - 5p^2 P_{3/2}$ | 0.00 | 1 | 0.142 | 1 | 24 | 7.00 |
| | 4215.52 | $5s^2 S_{1/2} - 5p^2 P_{1/2}$ | 0.00 | | -0.175 | | 10 | 6.91 |
| GeIII | | | | | | | | |
| | 4178.96 | $4s5s^3 S_1 - 4s5p^3 P_2$ | 19.66 | 2 | 0.341 | 5 | 63 | 6.36 |
| | 4260.85 | $4s5s^3 S_1 - 4s5p^3 P_1$ | 19.66 | | 0.108 | | 40 | 6.34 |
| | 4291.71 | $4s5s^3 S_1 - 4s5p^3 P_0$ | 19.66 | | -0.368 | | 10 | 6.14 |
| YIII | | | | | | | | |
| | 4039.602 | $4f^2 F_{7/2} - 5g^2 G_{9/2}$ | 12.53 | 3 | 1.005 |] | 5 | 21 |
| | 4039.602 | $4f^2 F_{7/2} - 5g^2 G_{7/2}$ | 12.53 | | -0.538 | | | |
| | 4040.112 | $4f^2 F_{5/2} - 5g^2 G_{7/2}$ | 12.53 | | 0.892 | | 21 | 6.24 |
| ZrIV | | | | | | | | |
| | 4137.435 | $5d^2 D_{3/2} - 6p^2 P_{3/2}^0$ | 18.18 | 4 | -0.625 | 5 | 10 | 6.20 |
| | 4198.265 | $5d^2 D_{5/2} - 6p^2 P_{3/2}^0$ | 18.23 | | 0.323 | | 86 | 6.43 |
| | 4317.081 | $5d^2 D_{3/2} - 6p^2 P_{1/2}^0$ | 18.18 | | 0.069 | | 64 | 6.49 |
| | 4569.247 | $5g^2 G_{7/2} - 6h^2 H_{9/2}^0$ | 25.65 | | 1.127 |] | 101 | 6.76 |
| | 4569.247 | $5g^2 G_{9/2} - 6h^2 H_{11/2}^0$ | 25.65 | | 1.216 | | | |

References:1. Brage et al. (1998), 2. Lang (1929), 3. Epstein & Reader (1975), 4. Reader & Acquista (1997), 5. this paper.

by explicit CI. However, transition data for the other ions has not been calculated to such accuracy, and therefore we undertook to provide that data ourselves.

For ions with valence electrons outside a number of closed subshells, there are three types of electron correlation which improve upon the HF approximation: valence shell correlation (with the core described as in the HF approximation); core-valence correlation (or core polarisation), in which the influence of the core on the valence electrons is included; core-core correlation. For monovalent ions, only the second and third of these effects occurs, in accordance with the work of Brage et al. (1998). We describe below our work on the three ions GeIII, YIII, ZrIV.

4.1 Ge III

This is the only ion considered here which has two valence electrons and therefore the only ion in which valence shell correlation must be included. Much work has been published on transitions amongst the $n = 4$ levels (for example, Chen & Cheng 2010), but almost nothing on transitions involving higher levels. We undertook our calculations of oscillator strengths using the configuration interaction code CIV3 (Hibbert 1975; Hibbert et al. 1991).

Relativistic effects, giving rise to fine-structure splitting, were included using the Breit-Pauli approximation, but all orbital optimisations were carried out in LS coupling. The radial functions of the orbitals are expressed in analytic form as sums of Slater-type orbitals. We used (in the absence of functions for GeIII) the radial functions of the ground state of GeII given by Clementi & Roetti (1974) but reoptimised the outer orbital functions $4s$ and $4p$ on the energy of the $4s4p^3 P^o$ state of GeIII. With these orbitals fixed, we optimised $5s$ and $5p$ on the energies of $4s5s^3 S$ and $4s5p^3 P^o$. Subsequent to this, we optimised $4d$ and $4f$ on the energy of $4s5p^3 P^o$ and $5d$ on $4s5s^3 S$. Valence-shell correlation was represented by constructing all possible configurations using these orbitals, but keeping a common core of filled subshells up to $3d$.

Core-valence correlation was represented by configurations with a single electron removed from $3d^{10}$ and replaced by $6p$ or $5f$, optimised on $4s5s^3 S$, with $4s5s$ replaced by $4s4p/4s5p$ and

vice versa. Core-core correlation is likely to have a very small effect on the oscillator strengths.

Our oscillator strengths (length form) are shown in Table 3, and are obtained using experimental wavelengths. The calculated energies agree with experiment to within 2%. The length and velocity forms also agree to within 5%. We also undertook the corresponding calculations in LS coupling and found approximately the same level of accuracy. We noted that, unlike the SrII work, core polarisation had only a small effect. This is partly because the orbitals of the transition ($5s$ and $5p$) are further from the core, and partly because the effective core experienced by these electrons also includes the $4s$ electron.

4.2 Y III

We proceeded in a similar manner for YIII: the starting point were the radial functions for the ground state of YII given by Clementi and Roetti (1974), and then reoptimised $4s$, $4p$ along with $4f$ on the $4s^2 4p^6 4f^2 F^o$ state, and then the $5g$ orbital function on the $^2 G$ state. In this case, no valence-shell correlation is possible, so core polarisation is the dominant correlation effect modelled explicitly by opening the $4p$ and $4s$ subshells. Specifically, we added to $4s^2 4p^6 5g^2 G$ the configurations $4s^2 4p^5 (4d6h + 4d4f + 4d5f)$ and $4s4p^6 (4f5p + 5p5f + 5p6h)$, with similar additions for the $^2 F^o$ state. We also added limited core-core correlation by means of configurations in which $4s$ is replaced by $4d$ in the main configurations, as well as $4p^6$ by $4p^4 4d^2$.

The resulting oscillator strengths are shown in Table 3. Again, calculated transition energies agree to within 4% of experiment. We consider that the oscillator strengths are accurate to better than 5%. As with GeIII, the effect of core polarisation is quite small, which is not surprising in view of the higher orbital angular momenta of the outer electron.

4.3 Zr IV

A similar process to that adopted for YIII was carried out for ZrIV, with the core orbitals chosen as those of the ZrII ground state, while

Table 4. Mean abundances ϵ_i for LS IV-14° 116.

| El. | LS IV-14° 116 | sdB ¹⁻⁵ | JL 87 ⁶ | He-sdB ⁷ | Sun ⁸ |
|-----|---------------|--------------------|--------------------|---------------------|------------------|
| H | 11.83 ± 0.07 | 12.0 | 11.6 | < 8.5 – 11.1 | 12.00 |
| He | 11.15 ± 0.05 | 7.9–11.4 | 11.3 | 11.5 | 10.93 |
| C | 8.04 ± 0.22 | 6.9–7.5 | 8.8 | 7.1–9.0 | 8.52 |
| N | 8.02 ± 0.20 | 7.4–7.6 | 8.8 | 8.3–8.7 | 7.92 |
| O | 7.60 ± 0.17 | 6.5–8.5 | 8.6 | 7.1–7.3 | 8.83 |
| Ne | < 7.6 | 6.5–8.5 | 8.31 | 8.2–8.5 | [8.08] |
| Mg | 6.85 ± 0.10 | 5.6–7.6 | 7.4 | 7.1–8.3 | 7.58 |
| Si | 6.32 ± 0.12 | 5.5–7.7 | 7.2 | 6.8–7.4 | 7.55 |
| Ar | < 6.5 | 6.0–9.0 | | | [6.40] |
| Sc | < 5.3 | 5.0–7.0 | | | 3.17 |
| Ti | < 6.0 | 5.3–9.0 | | | 5.02 |
| V | < 6.5 | 6.0–8.5 | | | 4.00 |
| Cr | < 7.0 | 5.5–8.0 | | | 5.67 |
| Fe | < 6.8 | 6.5–8.1 | | | 7.50 |
| Ge | 6.28 ± 0.12 | 1.5–5.5 | | | 3.41 |
| Sr | 6.96 ± 0.15 | | | | 2.97 |
| Y | 6.16 ± 0.10 | | | | 2.24 |
| Zr | 6.53 ± 0.24 | 2.7–4.9 | | | 2.60 |

1. Edelmann et al. (2003), 2. Geier et al. (2008), 3. Geier et al. (2010),
 4. O’Toole & Heber (2006), 5. Chayer et al. (2006), 6. Ahmad et al.
 (2007), 7. Naslim et al. (2010), 8. Grevesse & Sauval (1998)

Table 5. Abundance errors $\delta\epsilon_i$ due to representative errors in T_{eff} , $\log g$ and v_t

| Element | $\delta T_{\text{eff}} = 1000 \text{ K}$ | $\delta \log g = 0.2$ | $\delta v_t = 5$ |
|---------|--|-----------------------|------------------|
| C | +0.05 | +0.03 | -0.11 |
| N | -0.03 | +0.02 | -0.08 |
| O | -0.08 | -0.004 | -0.04 |
| Mg | -0.07 | -0.01 | -0.03 |
| Si | -0.13 | -0.02 | -0.04 |
| Ge | -0.13 | -0.02 | -0.05 |
| Sr | -0.24 | -0.08 | -0.01 |
| Y | -0.08 | -0.02 | -0.03 |
| Zr | +0.02 | +0.02 | -0.11 |

4s, 4p were reoptimised along with 5g on the ZrIV configuration 5g ²G and, with these core orbitals, 6h was optimised on the 6h ²H^o state. In a similar manner to YIII, orbitals 4d, 5s, 5p were introduced to allow for core polarisation. Two other orbitals, 4f and 7i, were introduced to allow for a more angular flexibility in the outer electrons. Again the effects of core polarisation are small, and length and velocity forms of the oscillator strengths agreed to around 3%.

A separate calculation was undertaken for the 5d–6p transitions. We reoptimised 4p along with 4d on the ²D state, and then with these functions optimised 5d, 5p and 6p on their respective states. To represent core-valence correlation, additional orbitals 5s, 7p, 6d, 4f were optimised to allow for configurations with one electron removed from the 4p subshell and 8p in order to polarise the 4s subshell. The calculated transition energies agreed very well with experiment (to within 1%). We estimate that the oscillator strengths are correct to within better than 10%. The effect of core polarisation was still small, principally due to the high *n*-values of the outer electrons.

5 ABUNDANCES

Individual line equivalent widths and abundances are given in Tables 3 and 2¹. Abundances are given in the form $\epsilon_i = \log n_i + c$ where $\log \sum_i a_i n_i = \log \sum_i a_i n_{i\odot} = 12.15$ and a_i are atomic weights. This form conserves values of ϵ_i for elements whose abundances do not change, even when the mean atomic mass of the mixture changes substantially.

Mean abundances for each element are given in Table 4. The errors given in Table 4 are based on the standard deviation of the line abundances about the mean or the estimated error in the equivalent width measurement. Systematic shifts attributable to errors in T_{eff} , $\log g$ and v_t are given in Table 5. The final best-fit spectrum using the adopted best-fit model and with the elemental abundances from Table 4 is shown in Fig. 5, together with identifications for all of the absorption lines in the model.

Table 4 also shows a representative range of abundances measured for normal sdB stars, for the intermediate helium sdB star JL 87, for helium-rich sdB stars and the Sun. In common with many helium-rich sdB stars, LS IV-14° 116 appears to be mildly metal-poor (Mg and Si are assumed as proxies for the mean metallicity). Relative to the Sun, nitrogen is unremarkable, but relative to Mg and Si, LS IV-14° 116 is arguably N-rich.

With a helium-to-hydrogen ratio of 0.2, LS IV-14° 116 falls well between the normal sdB stars, in which helium is strongly depleted, and the truly helium-rich sdB and sdO stars (Naslim et al. 2010; Stroeger et al. 2007). Only JL 87, with $n_{\text{H}}/n_{\text{He}} \approx 1$ might be comparable (Ahmad et al. 2007). However, JL 87 is strongly C- and N-rich, and shows no evidence for exotic species such as those described here.

Heavier elements, including argon and the iron-group elements scandium, titanium, vanadium, and chromium are frequently seen to be overabundant in H-rich sdB stars with higher effective temperatures (Geier et al. 2010). LS IV-14° 116 does not show any detectable lines due to these elements. We estimated upper limit abundances assuming a minimum observable equivalent width of 5mÅ (Table 4). Overabundances of Sc, Ti, V and Cr cannot be ruled out.

What is undeniable is that LS IV-14° 116 shows overabundances of Ge, Sr, Y and Zr which are unprecedented in any hot subdwarf and, possibly, in any other star (Sr, Y and Zr are only ≈ 2 dex overabundant in Przybylski’s star HD101065, although heavier elements do show 4 dex overabundances: Cowley et al. (2000); Shulyak et al. (2010)).

6 DISCUSSION

Both normal sdB stars and helium-rich subdwarfs are chemically peculiar. The former are depleted in helium and in other elements with $Z < 20$, but enriched in all elements $Z > 20$ except iron (O’Toole & Heber 2006; Geier et al. 2010). The consensus explanation is that chemical diffusion operates in an atmosphere where gravitational settling and radiative levitation compete to elevate ions to layers in which their specific opacities are maximised. Abundance information for helium-rich subdwarfs is less extensive (Naslim et al. 2010), but the absence of hydrogen and the enrichment of nitrogen and (sometimes) carbon point to nuclear-processed helium dominating the surface composition. A

¹ Abundances were calculated with improved model atmospheres, which give values different to those shown by Naslim et al. (2010)

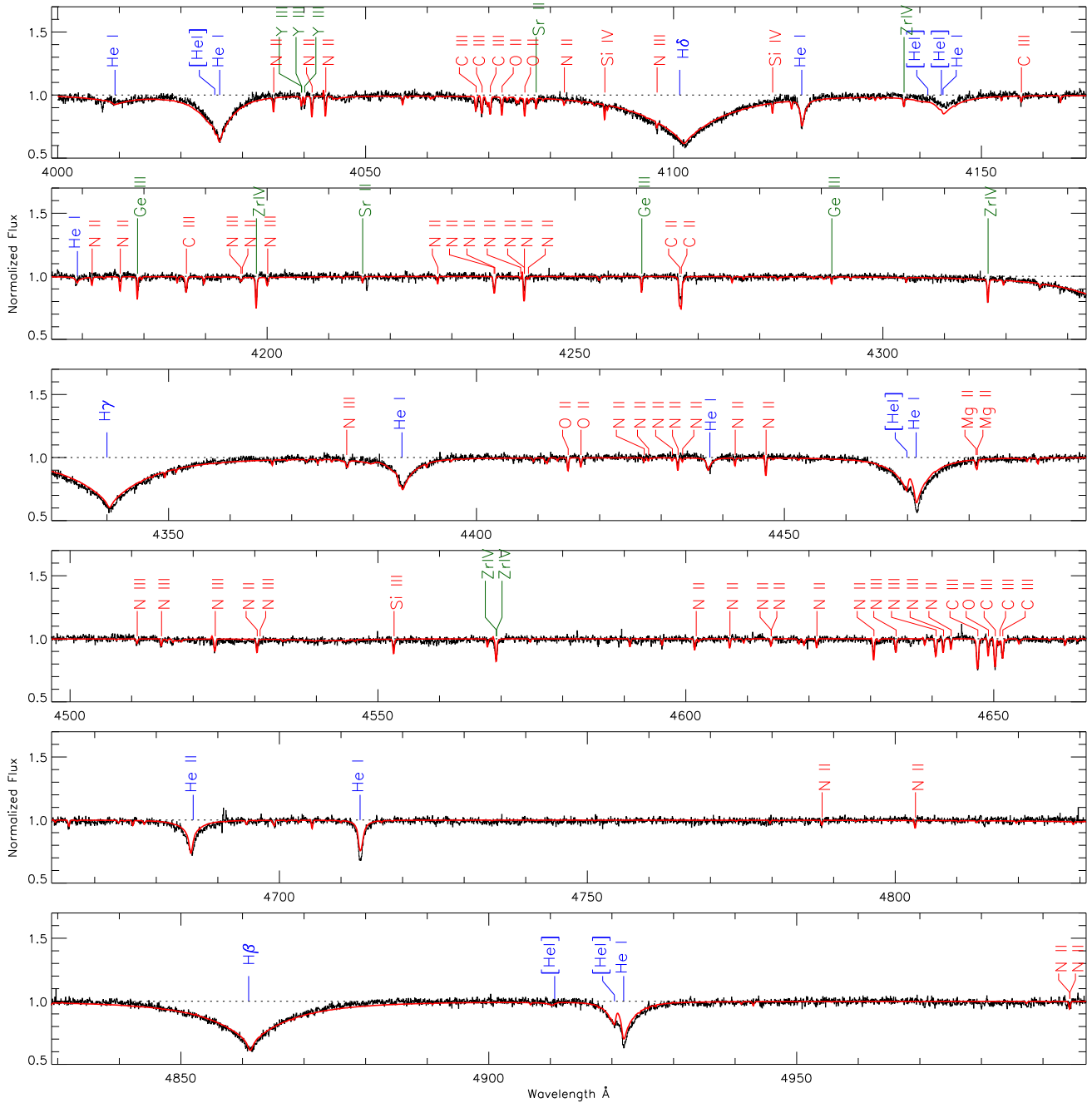


Figure 5. The merged AAT/UCLES spectrum of LS IV–14°116 along with the best FIT model of $T_{\text{eff}} = 34\,000$ K and $\log g = 5.50$. Abundances are as in Table 4.

few intermediate-helium sdB stars (with $0.1 < n_{\text{He}} < 0.9$) may be transition objects; if helium-rich sdBs are contracting towards the extended horizontal branch, intermediate-helium sdB stars may represent those stars in which diffusion has been effective sufficiently long to deplete the surface helium by a significant amount (Naslim et al. 2010).

6.1 Diffusion

However, chemical peculiarities of the magnitude seen on the surface of LS IV–14°116 demand a more sophisticated explanation.

Are they produced by some diffusion process which has led to extreme concentrations (*i.e.* clouds) in the line-forming region of the photosphere? Or are they a consequence of dredging-up heavily nuclear processed material from the intershell region of an AGB star?

LS IV–14°116 would barely qualify as “helium enriched” were it a main-sequence star. Only because sdB stars are generally so helium poor was it considered unusual in the first place. So the question of whether diffusion is responsible for other abundance anomalies is legitimate.

The elements Sr, Y, and Zr are recognized as products of s-process neutron-capture reactions which occur in the intershell in

asymptotic giant-branch (AGB) stars. They can appear on stellar surfaces following either third dredge-up on the AGB, a very late thermal pulse (*e.g.* FG Sge, V4334 Sge; Jeffery & Schönberner (2006); Asplund et al. (1999)), or as a consequence of a white dwarf merger, (*e.g.* V1920 Cyg, HD124448; Pandey et al. (2004)). The difficulties here are: (a) that none of these processes has previously been indicated to produce such a large excess; 1–2 dex is more common, (b) the absence of a characteristic carbon and/or oxygen excess, and (c) there is no evidence that LS IV-14° 116 is a post-AGB star in any sense.

Some abundance anomalies have been recognized as due to pollution from an external source. Dust-fractionated accretion from the interstellar medium tends to produce modest anomalies which are correlated with condensation temperature. This is not the case here. Accretion from the wind of a now unseen AGB companion can also be ruled out by the absence of a carbon and/or oxygen excess.

The principal advantage of the diffusion hypothesis is that it allows for a very high overabundance of a given species in a very narrow layer of the stellar atmosphere, but without requiring an additional source of that material providing that there is a commensurate depletion in other layers. Since the line-forming region of the stellar atmosphere (optical depth $0.001 \lesssim \tau \lesssim 0.1$) contains $\approx 4 \pm 1 \times 10^{-14} M_{\odot}$ compared with an estimated $7 \times 10^{-13} M_{\odot}$ for the total mass of the atmosphere ($\tau \lesssim 10$) and $\approx 0.001 M_{\odot}$ for the mass of the stellar envelope, the observed excess can be easily understood. It is important to note that overabundances of strontium and yttrium of up to 3 dex are well-documented in chemically-peculiar A (Ap) and mercury-manganese (HgMn) stars (Cowley & Hubrig 2008; Cowley et al. 2010; Dworetzky et al. 2008), where they are commonly attributed to radiatively-driven diffusion producing a strongly stratified atmosphere.

6.2 Variability

LS IV-14° 116 is known to be a low-amplitude light variable. Ahmad & Jeffery (2005) report two periods (1950 and 2900 s) and suggest these are due to non-radial g -mode oscillations of high radial order, since the periods are too long to be p -modes. A difficulty with this proposal is that g -modes are not predicted in sdB stars hotter than about 29 000 K (Jeffery & Schönberner 2006); with $T_{\text{eff}} = 34\,000$ K, LS IV-14° 116 sits in the middle of the sdB p -mode instability zone (Charpinet et al. 2001). Our three consecutive AAT spectra show no evidence of variability in line equivalent widths or radial velocity. This is probably a consequence of the low amplitude of the variability and the exposure times (1800 s) being long compared with the photometric periods.

There are two possible links between photometric variability and unusual chemical composition. The first regards the blue edge of the g -mode instability strip, which is very sensitive to the metal abundance in the driving zone (Jeffery & Saio 2006a). Reducing the hydrogen abundance also tends to destabilize pulsation (Jeffery & Saio 2006b) but, in this case, the hydrogen abundance is not sufficiently depressed to make a major difference. Should the overabundances seen in Ge, Sr, Y and Zr be reflected in other elements and also be continuous from the atmosphere to the driving zone at $\approx 2 \times 10^5$ K then, in all probability, there would be consequences for pulsational stability. However, as discussed above, there is no obvious source for such an excess throughout the stellar envelope. A strong requirement to demonstrate that the light variability of LS IV-14° 116 is due to pulsation is to investigate its radial-velocity behaviour. Observations which are sufficiently sen-

sitive to probe the behaviour of Ge, Sr, Y, and Zr lines, as well as the H and He lines would be indicative of differential motion within the stellar atmosphere.

The second possible link refers to observations of intermediate helium stars on the main sequence, sometimes known as Bp(He) stars. The class prototype is σ Ori E (Greenstein & Wallerstein 1958), a B2Vp star with a 1.1 d variation in light, a chemically-inhomogeneous surface and a strong magnetic field (Pedersen & Thomsen 1977; Thomsen 1974; Landstreet & Borra 1978). Strong magnetic fields are frequently associated with large abundance anomalies in early-type stars (Bohlender et al. 1987; Hunger & Groote 1999). In simple terms, a magnetic field radically alters the opacity of a given ion. Specifically, by splitting energy-level degeneracies, Zeeman splitting increases the line opacity in a direction parallel to the magnetic field lines. Consequently, radiative levitation preferentially leads to the greatest accumulation of susceptible elements in regions where the magnetic field is orthogonal to the stellar surface, *i.e.* at the magnetic poles. Such anomalies can be further exacerbated by fractionation in the stellar wind (Hunger & Groote 1999). Strong chemical anomalies appear as “spots” and can lead to light variability (Townsend et al. 2005).

We are not currently suggesting that LS IV-14° 116 is a classical Bp(He) star. Its surface gravity is too high and so a connection with the low-mass sdB stars seems more probable. However, we are suggesting that the same magnetically-driven physics could be responsible for the chemical anomalies. This suggestion can be tested. It requires that LS IV-14° 116 have a strong magnetic field, and it is possible that the light variations could be associated with chemical variability. High-resolution time-resolved spectroscopy would indicate whether the surface is chemically homogeneous. Simultaneous photometry would demonstrate any link to light variability. Spectropolarimetry would indicate a magnetic field.

7 CONCLUSION

LS IV-14° 116 is an intermediate helium-rich subdwarf B star, with a gravity slightly lower than that of normal sdB stars, and a surface helium abundance of about 16% by number. Taking silicon and magnesium as proxies for the mean metal abundance, it is slightly metal poor (-0.8 dex) relative to the Sun. Since nitrogen is approximately solar, and carbon and oxygen are 0.4 and 1.1 dex subsolar respectively, the excess helium is overabundant, it is possible that the surface consists of a mixture of hydrogen with CNO-processed helium. How diffusion affects C, N and O is not clear. Neither is it currently known whether LS IV-14° 116 is a single star or has an undetected binary companion.

In conjunction with observations of other helium-rich sdB stars (Naslim et al. 2010), it might be argued that LS IV-14° 116 was formed from either a helium white dwarf merger, or a late helium-flash episode, in which such a mixture could arise. Whether the observed helium/hydrogen ratio represents the relative contributions of the original material is difficult to establish; radiative levitation may already have caused a substantial fraction of the helium to sink as the star contracts towards the zero-age extended horizontal branch.

What makes LS IV-14° 116 remarkable, and distinct from any other hot subdwarf, whether helium-rich or not, is the presence of lines due to germanium (GeIII), strontium (SrII), yttrium (YIII) and zirconium (ZrIV) in its optical spectrum. Measurements of these lines translate into overabundances of up to four orders

of magnitude of these elements in the line-forming region of the photosphere.

Since a nuclear origin for such overabundances seems unlikely, it is argued that they arise due to radiatively-driven diffusion, where elements accumulate in layers of high specific opacity and where radiative and gravitational forces are in equilibrium. It is conjectured that a strong magnetic field might be responsible for the extreme overabundances observed in this case. How the unusual chemistry is linked to the photometric variability remains to be established.

ACKNOWLEDGMENTS

This paper is based on observations obtained with the Anglo-Australian Telescope. The authors are grateful to Drs Amir Ahmad and Timur Şahin who made the observations and reduced the data. The Armagh Observatory is funded by direct grant from the Northern Ireland Dept of Culture Arts and Leisure.

References

- Ahmad A., Behara N. T., Jeffery C. S., Sahin T., Woolf V. M., 2007, *A&A*, 465, 541
- Ahmad A., Jeffery C. S., 2003, *A&A*, 402, 335
- Ahmad A., Jeffery C. S., 2004, *Ap&SS*, 291, 253
- Ahmad A., Jeffery C. S., 2005, *A&A*, 437, L51
- Ahmad A., Jeffery C. S., 2006, *Baltic Astronomy*, 15, 139
- Asplund M., Lambert D. L., Kipper T., Pollacco D., Shetrone M. D., 1999, *A&A*, 343, 507
- Becker S. R., Butler K., 1988, *A&A*, 209, 244
- Becker S. R., Butler K., 1989, *A&A*, 235, 326
- Becker S. R., Butler K., 1990, *A&A*, 201, 232
- Blanchette J., Chayer P., Wesemael F., Fontaine G., Fontaine M., Dupuis J., Kruk J. W., Green E. M., 2008, *ApJ*, 678, 1329
- Bockasten K., 1955, *Ark. Fys.*, 9, 457
- Bohlender D. A., Landstreet J. D., Brown D. N., Thompson I. B., 1987, *ApJ*, 323, 325
- Brage T., Wahlgren G. M., Johansson S. G., Leckrone D. S., Proffitt C. R., 1998, *ApJ*, 496, 1051
- Butler K., 1984, PhD Thesis, University College London
- Charpinet S., Fontaine G., Brassard P., 2001, *Publ. Astron. Soc. Pac.*, 113, 775
- Chayer P., Fontaine M., Fontaine G., Wesemael F., Dupuis J., 2006, *Baltic Astronomy*, 15, 131
- Chen M. H., Cheng K., 2010, *J. Phys. B: Atom. Molec. Opt. Phys.*, 43, 074019
- Clementi E., Roetti C., 1974, *Atom. Data Nucl. Data Tables*, 14, 177
- Cowley C. R., Hubrig S., 2008, *MNRAS*, 384, 1588
- Cowley C. R., Hubrig S., Palmeri P., Quinet P., Biémont É., Wahlgren G. M., Schütz O., González J. F., 2010, *MNRAS*, 405, 1271
- Cowley C. R., Ryabchikova T., Kupka F., Bord D. J., Mathys G., Bidelman W. P., 2000, *MNRAS*, 317, 299
- Dworetzky M. M., Dyer A., Persaud J. L., 2008, *Contributions of the Astronomical Observatory Skalnaté Pleso*, 38, 141
- Edelmann H., Heber U., Hagen H., Lemke M., Dreizler S., Napiwotzki R., Engels D., 2003, *A&A*, 400, 939
- Epstein G. L., Reader J., 1975, *Opt. Soc. Am.*, 65, 310
- Geier S., Heber U., Edelmann H., Morales-Rueda L., Napiwotzki R., 2010, *Ap&SS*, p. 109
- Geier S., Heber U., Napiwotzki R., 2008, in U. Heber, C. S. Jeffery, & R. Napiwotzki ed., *Hot Subdwarf Stars and Related Objects Vol. 392 of Astronomical Society of the Pacific Conference Series, Metal Abundances of Subdwarf B Stars from SPY – a Pattern Emerges*. p. 159
- Green R. F., Schmidt M., Liebert J., 1986, *ApJS*, 61, 305
- Greenstein J. L., Wallerstein G., 1958, *ApJ*, 127, 237
- Grevesse N., Biémont E., Hannaford P., Lowe R., 1991, *Proc. Conf. on Upper Main Sequence Chemically Peculiar Stars*, 47, 211
- Grevesse N., Sauval A. J., 1998, *Space Science Reviews*, 85, 161
- Hardorp J., Scholz M., 1970, *ApJS*, 19, 193
- Heber U., 1986, *A&A*, 155, 33
- Hibbert A., 1975, *Computer Physics Communications*, 9, 141
- Hibbert A., 1976, *J.Phys.B*, 9, 2805
- Hibbert A., Glass R., Froese Fischer C., 1991, *Computer Physics Communications*, 64, 455
- Hunger K., Groote D., 1999, *A&A*, 351, 554
- Jeffery C. S., Heber U., Hill P. W., Dreizler S., Drilling J. S., Lawson W. A., Leuenhagen U., Werner K., 1996, in Jeffery C. S., Heber U., eds, *Hydrogen Deficient Stars Vol. 96 of Astron. Soc. Pac. Conf. Ser.*, A catalogue of hydrogen-deficient stars. p. 471
- Jeffery C. S., Saio H., 2006a, *MNRAS*, 371, 659
- Jeffery C. S., Saio H., 2006b, *MNRAS*, 372, L48
- Jeffery C. S., Schönberner D., 2006, *A&A*, 459, 885
- Kilkenny D., Pauls L., 1990, *MNRAS*, 244, 133
- Landstreet J. D., Borra E. F., 1978, *ApJ*, 224, L5
- Lang R., 1929, *Phys.Rev*, 34, 697
- Migdalek J., Bayliss W., 1979, *J. Phys. B*, 12, 1113
- Moehler S., Richtler T., de Boer K. S., Dettmar R. J., Heber U., 1990, *A&AS*, 86, 53
- Naslim N., Jeffery C., Ahmad A., Behara N., Şahin T., 2010, *MNRAS*, In press
- O’Toole S. J., 2004, *A&A*, 423, L25
- O’Toole S. J., Heber U., 2006, *A&A*, 452, 579
- Pandey G., Lambert D. L., Rao N. K., Jeffery C. S., 2004, *ApJ*, 602, L113
- Pedersen H., Thomsen B., 1977, *A&AS*, 30, 11
- Pereira C., 2010, PhD thesis, Queens University Belfast
- Reader J., Acquista A., 1997, *Opt. Soc. Am. B*, 14, 1328
- Shulyak D., Ryabchikova T., Kildiyarova R., Kochukhov O., 2010, *ArXiv 1004.0246*
- Stroeer A., Heber U., Lisker T., Napiwotzki R., Dreizler S., Christlieb N., Reimers D., 2007, *A&A*, 462, 269
- Thomsen B., 1974, *A&A*, 35, 479
- Townsend R. H. D., Owocki S. P., Groote D., 2005, *ApJ*, 630, L81
- Viton M., Deleuil M., Tobin W., Prevot L., Bouchet P., 1991, *A&A*, 242, 175
- Wiese W., Smith M., Glennon 1966, *National Bureau of Standards (USA) Publs*, I-II
- Yan C., Taylor K., Seaton M., 1987, *J.Phys.B*, 20, 6399